

Size effect and surface tension measurements in Ni and Co nanowires

Kleber R. Pirota,^{1,*} Elvis L. Silva,^{2,3} Daniela Zanchet,³ David Navas,⁴ Manuel Vázquez,⁴ Manuel Hernández-Vélez,¹ and Marcelo Knobel²

¹*Departamento de Física Aplicada, Universidad Autónoma de Madrid, 28049 Madrid, Spain*

²*Instituto de Física Gleb Wataghin, Universidade Estadual de Campinas, Campinas São Paulo 13083-970, Brazil*

³*Laboratório Nacional de Luz Síncrotron, Caixa Postal 6192, Campinas São Paulo 13084-971, Brazil*

⁴*Instituto de Ciencia de Materiales, CSIC, 28049 Madrid, Spain*

(Received 29 August 2007; revised manuscript received 2 November 2007; published 26 December 2007)

The effect of reduced size on the mechanical and elastic properties measured on 35 nm diameter Ni and Co nanowires is presented and discussed. The stresses induced in the nanowires due to the different thermal expansion constants of the metal and alumina change the magnetic properties of the nanowires, allowing one to measure the effective Young's modulus and the surface tension of the nanowires by means of simple magnetometry. The Young's modulus of the longer nanowire is higher than that of the shorter one that is comparable to its bulk value. This effect is successfully attributed to surface tension effects.

DOI: [10.1103/PhysRevB.76.233410](https://doi.org/10.1103/PhysRevB.76.233410)

PACS number(s): 62.25.+g, 61.46.-w, 62.20.Dc

Metallic nanowires are among the most attractive nanometer-sized materials because of their unique properties that lead to a huge variety of applications, including interconnections in nanoelectronics; spintronics based devices; and magnetic, chemical, optical, or biological sensors.¹⁻⁵ Many physical properties of nanowires, and particularly the magnetic behavior, strongly depend on the mechanical stresses that such nanowires are subjected to. However, at the nanoscale the mechanical behavior of materials is often different from that at the macroscopic scale since size effects may control the plastic and elastic properties. In a classical work, Shuttleworth clarified the concept of surface tension of solids and its difference from the solid's surface free energy.⁶ For liquids, the surface free energy and tension are equal. For crystals, the surface energy is different from the surface tension. It is worth noting that there are very few experimental measurements of surface tension of solids, and most values reported in the literature arise from theoretical calculations. Such calculations predict that surface tension values are of the same order of magnitude of the surface energy values.⁷ Wessermann and Vermaak have experimentally determined the surface tension value for silver from the measurement of the lattice contraction in small Ag spheres as a function of their radius by electron diffraction.⁸ More recently, Web III *et al.* determined, by molecular dynamic simulations,⁹ the liquid-vapor surface tension of Al, Ni, Cu, Ag, and Au. Here, the effect of reduced size on the mechanical and elastic properties measured on 35 nm diameter Ni and Co nanowires (length ranging between 530 and 2250 nm) embedded into an alumina matrix is presented and discussed. The stresses induced in the nanowires due to the different thermal coefficient constants of the metal and alumina originates significant changes in the magnetic properties of the nanowires. This allows one to measure the effective Young's modulus and estimate the surface tension of the nanowires by means of simple magnetometry. Most outstanding, in the present work we found that Young's modulus varies with the length of the nanowire, which we have correlated to a surface tension effect.

The metal nanowires were prepared by filling the ordered porous array of an alumina membrane. For all the magnetic

measurements presented here, the nanowires were kept embedded in the matrix, as deposited. The polycrystalline morphological structure of the electrodeposited nanowires was determined by x-ray diffraction and high-resolution transmission electron microscopy (HRTEM) measurements.

The fabrication of the anodized alumina membranes was done following the two-step anodization process.¹¹ The anodization procedure was done using 0.3M of oxalic acid solution as electrolyte. The anodization voltage was kept at 40 V and the electrolyte temperature at 2 °C. The first anodization time, which determines the final hexagonal order degree, was 24 h for all samples. The second anodization time was 2 h for all the samples, given a total porous length of about 4.5 μm . A final self-assembled array of nanopores is obtained having long range ordering of hexagonal symmetry. The Ni and Co nanowires growth into the pores of the anodized alumina membrane (AAM) were carried out in a special homemade electrochemical cell by a pulsed electrodeposition method, using the respective well known Watts bath giving uniform arrays of nanowires with a diameter of 35 nm, arranged with hexagonal symmetry with a lattice constant (or internanowire distance) of 105 nm. The electrodeposition time, that determines the nanowires length, was varied between 15 and 60 min. The length of the shortest nanowires, corresponding to 15 min of electrodeposition time resulted to be 530 nm in length while the longest one, for 60 min electrodeposition, resulted in a length of 2250 nm [estimated by the deposition time and confirmed by scanning electron microscopy, as one can see in Figs. 1(a)–1(c), for three samples used in this experiment]. Figure 1(a) corresponds to 15 min of Ni electrodeposition that gives approximately 530 nm of nanowire length. Figure 1(b) shows a 1130 nanowire length (30 min electrodeposition) and Fig. 1(c) corresponds to a 45 min electrodeposition (about 1700 nm length). This is in good agreement with our electrodeposition time calibration of approximately 37 nm length nanowire per min deposition. Morphological studies were performed by high-resolution scanning electron microscopy (LNLS, Brazil). The magnetization measurements were performed in a Quantum Design XL7 superconducting quantum interference device magnetometer.

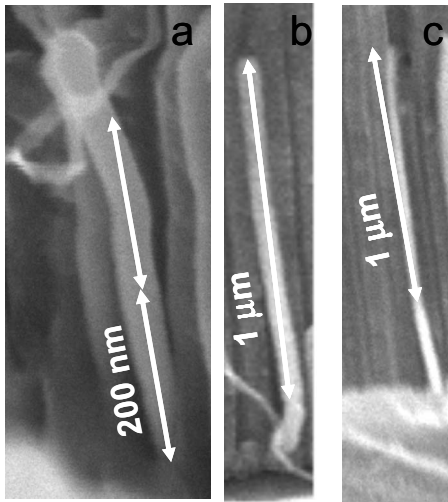


FIG. 1. Nanoporous alumina template. HRSEM (high resolution scanning electron microscopy) image of three different studied Ni nanowires: (a) 15 min, (b) 30 min, and (c) 45 min of electrodeposition time.

Figure 2 shows the hysteresis loops for the Ni nanowires with 530 nm length at 300 and 4 K, as an example. Hysteresis loops with applied magnetic field parallel and perpendicular to the nanowire axes are shown to identify the easy anisotropy magnetic axis. As can be clearly seen, there is a significant change in the magnetic anisotropy of the nanowires when the temperature increases from 4 to 300 K, indicating a change of the magnetic easy axis from perpendicular towards parallel to the nanowire axis. This phenomenon is observed for all studied lengths. This trend is in agreement with previous data observed in similar systems.¹² In addition, several studies have shown that the stresses seem to dominate the increase of a transverse magnetic anisotropy when temperature is decreased.¹³

Figures 3(a)–3(d) show the temperature behavior of the saturation field, defined as the magnetic field value to nearly saturate the sample in a given direction, obtained from hysteresis loops taken at different temperatures. As in Fig. 2, results are for the applied magnetic field both perpendicular and parallel to the nanowire axis. We define the crossover temperature as the temperature at which the saturation fields

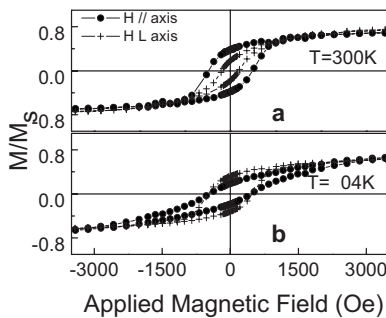


FIG. 2. Magnetization curves. Comparison of the hysteresis loops for the Ni samples with 530 nm nanowire length for two temperature values (300 and 4 K).

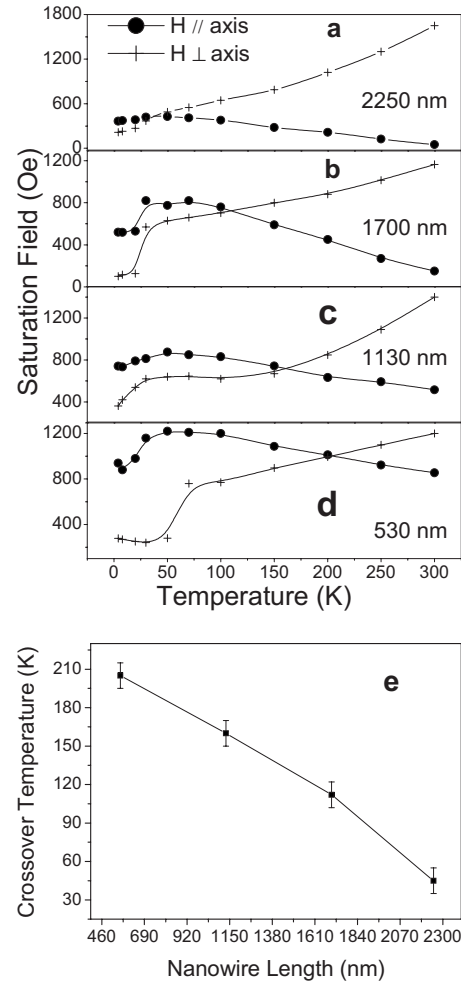


FIG. 3. Saturation field behavior and crossover temperature. Temperature dependence of the saturation field for Ni nanowires with lengths of 2250 (a), 1700 (b), 1130 (c), and 530 nm (d), respectively. The crossover temperature is considered as the temperature below which the magnetization is preferably oriented transversal to the nanowire axes (e).

for parallel and perpendicular configurations intersect (below the crossover temperature the magnetic easy axis is perpendicular to the wire axis). As can be observed in Figs. 3(a)–3(d), all samples present a clear crossover temperature, which is closer to room temperature for the 530 nm long Ni nanowires and shifts towards lower temperatures as the nanowire length increases. These results are summarized in Fig. 3(e).

The effective anisotropy constant, K_{eff} , can be evaluated from the experimental magnetization loops as the difference between the magnetic fields required to saturate the magnetization parallel and perpendicular to the wire axis:¹⁴

$$K_{eff} = \frac{1}{2} \mu_0 M_s (H_s^{perp} - H_s^{par}), \quad (1)$$

where $\mu_0 M_s$ is the saturation magnetization and H_s^{perp} and H_s^{par} are the values of the applied magnetic fields necessary to saturate the magnetization perpendicular and parallel to

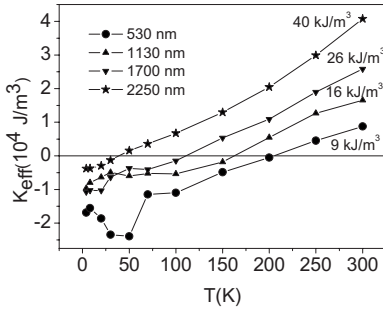


FIG. 4. Temperature dependence of the effective magnetic anisotropy constant, for the arrays of Ni nanowires, with different lengths.

the nanowires axis, respectively. The temperature dependence of the effective anisotropy constant for the Ni nanowire arrays is observed in Fig. 4, where $\mu_0 M_s = 0.64$ T has been considered. The points where K_{eff} changes sign correspond to the crossover temperatures mentioned above. The values labeling the curves are the values for the anisotropy constant at 300 K. Those values represent the energy needed to be overcome to change the magnetic anisotropy configuration of the nanowires. As discussed elsewhere^{15,16} magnetoelastic energy dominates in this system. The induced magnetoelastic anisotropy arises from the difference between the thermal expansion coefficients of embedded nanowires and alumina. The induced stresses originating from this effect, coupled to the negative magnetostriction of Ni, lead to a magnetoelastic anisotropy that makes the magnetic easy axis of the nanowires change from the parallel to perpendicular direction as the temperature is decreased. Thus the above defined effective anisotropy constant, K_{eff} , owing to its magnetoelastic origin, can be expressed as

$$K_{\sigma} = \frac{3}{2} \lambda_s \sigma \Leftrightarrow K_{eff}, \quad (2)$$

where λ_s is the saturation magnetostriction constant of polycrystalline Ni taken as -33×10^{-6} ,¹⁷ and σ is an effective induced axial stress, connected to the longitudinal strain as

$$\sigma = E_{eff} \frac{\Delta l}{l}, \quad (3)$$

where E_{eff} is the effective Young's modulus of the nanowires and $\Delta l/l$ is the corresponding strain. Generally speaking, the thermal expansion coefficient is temperature dependent, and therefore the mentioned strain should be calculated using the following integral:

$$\frac{\Delta l}{l} = \int_{T_i}^{T_f} \Delta \alpha(T) dT, \quad (4)$$

where T_i is 300 K, and T_f is taken as the crossover temperature. $\Delta \alpha(T)$ is the temperature dependent difference $\alpha_{Ni,Co} - \alpha_{alumina}$. To perform such an analytical integral, a 9^o polynomial fit was previously performed in the curve $\Delta \alpha(T)$ with data of Ni, Co, and alumina taken from the

TABLE I. Effective tensile induced stress σ , effective strain $\Delta l/l$, and the effective Young's modulus E_{eff} , for Ni nanowires with different lengths.

| Length (nm) | σ (Pa) | $\Delta l/l \times 10^7$ | E_{eff} |
|-------------|--------------------|--------------------------|-----------------------|
| 530 | -1.7×10^8 | -7550.43 | 2.3×10^{11} |
| 1130 | -3.2×10^8 | -10 527.5 | 3.0×10^{11} |
| 1700 | -5.0×10^8 | -13 989.4 | 3.6×10^{11} |
| 2250 | -7.8×10^8 | -16 694.4 | 4.68×10^{11} |

literature.^{18,19} The obtained results for all Ni samples are summarized in Table I.

The induced strain in the nanowires actually denotes an increase or decrease of its length, resulting in an increase or decrease of its cross section. Surface tension effects can be considered to account for the observed results. Following the same reasoning as Cuenot *et al.*,¹⁰ the effective Young's modulus, E_{eff} , is connected with the bulk's one, E_{bulk} , according to the following relation that takes into account also the material's Poisson's ratio and surface tension:

$$E_{eff} = E_{bulk} + \frac{8}{5} \gamma (1 - \nu) \frac{L^2}{D^3}, \quad (5)$$

where γ is the surface tension of the Ni nanowires, ν is their Poisson's ratio taken as 0.33,¹⁷ and L^2/D^3 is the squared nanowires length divided by the third power of its diameter. From Eq. (5) and plotting the effective Young's modulus E_{eff} versus the geometrical parameter L^2/D^3 , a linear relation is expected where a nonzero intercept with the ordinate axis gives the bulk's Young's modulus E_{bulk} . From linear fitting one can get the contribution due to surface tension effect γ as shown in Fig. 5 for the Ni nanowires. The extrapolated Ni bulk's Young's modulus is $(2.2 \pm 0.4) \times 10^{11}$ Pa, comparable with the values reported in the literature for magnetically saturated Ni, 2.22×10^{11} Pa,¹⁷ while the value of the surface tension for the Ni nanowires was of 2.0 ± 0.4 J/m², determined with a Poisson's ratio of 0.33.

To the best of our knowledge, no data are available for the surface tension of Ni in this temperature range; however, it can be noticed that the obtained surface tension of Ni is comparable to the published value of the surface tension in the temperature range between 1800 and 2100 K

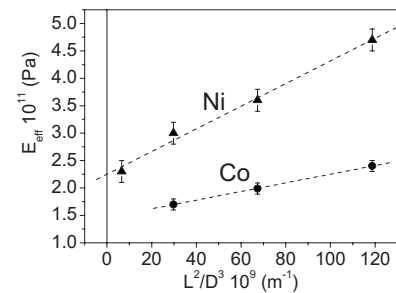


FIG. 5. Effective Young's modulus as a function of the geometrical parameter, L^2/D^3 , for the Ni and Co nanowire arrays.

(1.6 J/m^2),⁹ as well as to the surface energy calculated by Aldén *et al.*²⁰ (2.7 J/m^2).

The same procedure was also applied to the Co nanowire arrays. In this case, a value of -55×10^{-6} was taken for the polycrystalline Co saturation magnetostriction constant.¹⁷ The obtained effective Young's modulus E_{eff} is presented in Fig. 5. The Co bulk's Young's modulus was found to be $(1.6 \pm 0.2) \times 10^{11} \text{ Pa}$, comparable with the few values reported in the literature, $2.0 \times 10^{11} \text{ Pa}$.¹⁷ The value of the surface tension for the Co nanowires was of $0.8 \pm 0.2 \text{ J/m}^2$ [with a Poisson's ratio of 0.31 (Ref. 17)] which is about one-half of that for the Ni. To the best of our knowledge, as in the case of Ni, no data are available for the surface tension of Co in those experimental conditions. Aldén *et al.*²⁰ discussed the anomalous low surface energy values for some magnetic 3d metals. In the case of magnetic Co, the system gives access to an extra degree of freedom which in the surface region can be utilized to further minimize the energy difference between

a bulk and a surface atom, an effect that is not observed in the case of Ni. As a result, the Co surface energy may be strongly affected and appear anomalously lower than in the case of Ni. Another effect that might be relevant in the Co case is the larger magnetocrystalline anisotropy and detailed studies are on the way to further address this issue.

In conclusion, the Young's modulus and the surface tension of metallic Ni and Co nanowires with different lengths ranging between 530 and 2250 nm (fixed 35 nm diameter) was measured using a very simple magnetic characterization. For longer nanowires, the measured Young's modulus significantly differs from that of the bulk materials. Calculations of an effective Young's modulus taking into account the surface effects shows that the observed increase of the Young's modulus with the increase of length is well-explained by surface tension effects. This model allows one the calculation of the intrinsic Young's modulus and the surface tension of the probed material from the measured effective modulus.

*Corresponding author. Universidad Autónoma de Madrid, Facultad de Ciencias, C-XII, Departamento de Física Aplicada, C-XII, Ctra. Colmenar Viejo, Km. 15, 28049 Cantoblanco, Madrid, Spain. kleber.pirota@uam.es; FAX: 0034 914973969.

¹C. A. Ross, *Annu. Rev. Mater. Res.* **31**, 203 (2001).

²Y. Cui, Q. Wei, H. Park, and C. M. Lieber, *Science* **293**, 1289 (2001).

³S. Melle, J. L. Menéndez, G. Armelles, D. Navas, M. Vazquez, and K. Nielsh, *Appl. Phys. Lett.* **83**, 4547 (2003).

⁴S. Christiansen and U. Gösele, *Nat. Mater.* **3**, 357 (2004).

⁵G. Zheng, F. Patolsky, Y. Cui, W. U. Wang, and C. M. Lieber, *Nat. Biotechnol.* **23**, 1294 (2005).

⁶R. Shuttleworth, *Proc. Phys. Soc., London, Sect. A* **63**, 444 (1950).

⁷R. C. Camarata, *Prog. Surf. Sci.* **46**, 1 (1994).

⁸H. J. Wassermann and J. S. Vermaak, *Surf. Sci.* **22**, 164 (1970).

⁹E. B. Web III and G. S. Grest, *Phys. Rev. Lett.* **86**, 2066 (2001).

¹⁰S. Cuenot, C. Fretigny, S. Demoustier-Champagne, and B. Nysten, *Phys. Rev. B* **69**, 165410 (2004).

¹¹H. Masuda and K. Fukuda, *Science* **268**, 1466 (1995).

¹²M. Vazquez, K. R. Pirota, J. Torrejón, D. Navas, and M. Hernandez-Velez, *J. Magn. Magn. Mater.* **294**, 174 (2001).

¹³Y. S. Kim and S. C. Shin, *Phys. Rev. B* **59**, R6597 (1999).

¹⁴J. Jorritsma and J. A. Mydosh, *J. Appl. Phys.* **84**, 901 (1998).

¹⁵E. L. Silva, W. C. Nunes, M. Knobel, J. C. Denardin, D. Zanchet, K. R. Pirota, D. Navas, and M. Vazquez, *Physica B* **384**, 22 (2006).

¹⁶A. Kumar, S. Fahler, H. Schlorb, K. Leistner, and L. Schultz, *Phys. Rev. B* **73**, 064421 (2006).

¹⁷R. M. Bozorth, *Ferromagnetism* (Van Nostrand, New York, 1951).

¹⁸G. K. White, *Proc. Phys. Soc. London* **86**, 159 (1965).

¹⁹H. Hayashi, M. Watanabe, and H. Inaba, *Thermochim. Acta* **359**, 77 (2000).

²⁰M. Aldén, H. L. Skriver, S. Mirbt, and B. Johansson, *Phys. Rev. Lett.* **69**, 2296 (1992).